

Identification of RO4597014, a Glucokinase Activator Studied in the Clinic for the Treatment of Type 2 Diabetes

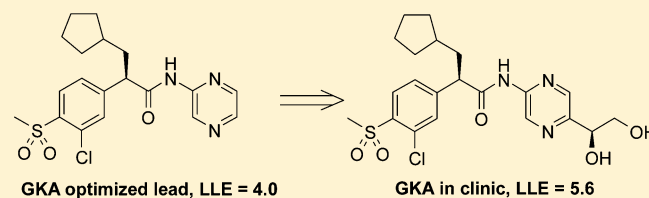
Yimin Qian,^{*,†} Wendy L. Corbett,[†] Steven J. Berthel,[†] Duk Soon Choi,[‡] Mark T. Dvorozniak,[§] Wanping Geng,^{||} Paul Gillespie,[†] Kevin R. Guertin,[†] Nancy-ellen Haynes,[†] Robert F. Kester,[†] Francis A. Mennona,[†] David Moore,^{||} Jagdish Racha,^{||} Roumen Radinov,[⊥] Ramakanth Sarabu,[†] Nathan R. Scott,[†] Joseph Grimsby,[§] and Navita L. Mallalieu[#]

[†]Departments of Discovery Chemistry, [‡]Pharmaceutical and Analytical Research, [§]Metabolic and Vascular Diseases, ^{||}Drug Metabolism and Pharmacokinetics, [⊥]Process Research, [#]Clinical Pharmacology, Hoffmann-La Roche, 340 Kingsland Street, Nutley, New Jersey 07110, United States

Supporting Information

ABSTRACT: To resolve the metabolite redox cycling associated with our earlier clinical compound **2**, we carried out lead optimization of lead molecule **1**. Compound **4** showed improved lipophilic ligand efficiency and demonstrated robust glucose lowering in diet-induced obese mice without a liability in predictive preclinical drug safety studies. Thus, it was selected as a clinical candidate and further studied in type 2 diabetic patients. Clinical data suggests no evidence of metabolite cycling, which is consistent with the preclinical

KEYWORDS: Glucokinase activator, type 2 diabetes, lipophilic ligand efficiency, metabolite, redox cycling



profiling of metabolism.

Glucokinase (GK) catalyzes the phosphorylation of glucose to glucose-6-phosphate. GK is widely accepted as a glucose sensor, and compounds that activate GK could lead to a potential therapy for type 2 diabetes.¹ Since our discovery of phenylacetamides as potent allosteric GK activators,^{2,3} GK activators (GKAs) with chemical structures closely related to the phenylacetamide scaffold or from completely different chemical classes have been reported.^{4–12} Recently, we reported that **1**, a lead molecule with robust *in vivo* efficacy, inactivated cytochrome P450 3A4 (CYP3A4) in a time-dependent manner, blocked the human-Ether-à-go-go-Related Gene (hERG) potassium channel and increased the duration of the action potential in the rabbit Purkinje fiber assay. After extensive metabolite profiling of **1** from *in vitro* and *in vivo* studies, **2** (Piragliatin) was identified as an active metabolite without the liability of hERG inhibition or CYP3A4 time-dependent inactivation (TDI).¹³ This molecule was further developed and evaluated in diabetic patients.

Although replacing the cyclopentane moiety in **1** with a cyclopentanone in **2** resolved issues of hERG inhibition and CYP3A4 inactivation, **2** was observed to undergo ketone/alcohol redox cycling between **2** and **3** (Figure 1) from both *in vitro* and *in vivo* metabolism studies. In searching for a backup molecule, our goal was to identify potent GK activators in the aminopyrazine phenylacetamide chemical class devoid of metabolite cycling. Herein, we report our lead optimization of **1**, which culminated in the identification of **4** (RO4597014), a potent GK activator that entered clinical studies in type 2 diabetic patients.

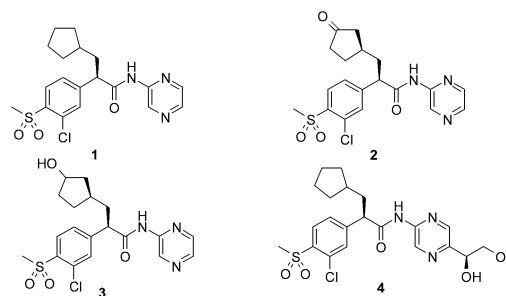


Figure 1. Chemical structures of **1**–**4**.

In order to resolve the issue of metabolite cycling between **2** and **3**, we initially focused on the modification of the cycloalkyl side chain. As illustrated in Table 1, significant loss of GK activation potency ($SC_{1.5}$, stimulation concentration required to achieve GK activity 150% of the control) was observed when the cyclopentane fragment was replaced with 4-tetrahydropyran or 3-tetrahydrofuran (**7** and **8**). To resolve the hERG inhibition and CYP3A4 inactivation associated with **1**, we investigated less hydrophobic groups at the R1 and R2 positions. However, these modifications caused a decrease in GK activation potency (compound **6** in Table 1, and compounds **42**–**49** in Table S1 of the Supporting Information). Structure–activity relationships (SARs) from Table 1 and Table S1, Supporting

Received: January 23, 2013

Accepted: March 7, 2013

Published: March 7, 2013

Table 1. GK Activation Potency, Effects on Inactivating CYP3A4, Inhibition of hERG, and in Vivo Efficacy in Lowering Blood Glucose in C57 Mice by Compounds 1, 4, and 9–24

6: R1 = OMe, R2 = cyclopentyl
7: R1 = Cl, R2 = 4-tetrahydropyran
8: R1 = Cl, R2 = 3-tetrahydrofuran
1, 4 and 9–24

entry	R3	SC _{1.5} (μM) ^a	hERG inhib (%) ^b	CYP 3A4 TDI (%) ^c	in vivo glucose change (%) ^d	LLE ^e	entry	R3	SC _{1.5} (μM) ^a	hERG inhib (%) ^b	CYP 3A4 TDI (%) ^c	in vivo glucose change (%) ^d	LLE ^e
1	H	0.11	59	60	-53	4.0	16		0.022	46	30	-46	5.9
6		1.9	36	ND	ND	3.7	17		0.056	43	16	-48	4.8
7		1.4	8.1	ND	-5.6	4.7	18		0.11	86	18	-46	4.4
8		3.6	ND	ND	ND	4.8	19		0.14	53	45	-49	4.4
9		0.054	70	21	-26	3.1	20		0.075	39	23	-45	5.7
10		0.40	27	<1.0	-26	4.3	21		0.13	40	16	-43	4.7
11		0.19	22	22	-38	4.5	4		0.26	22	8.3	-44	5.6
12		0.30	23	38	-29	4.3	22		0.31	19	5.6	-44	4.8
13		0.037	50	28	-53	5.6	23		0.41	37	ND	-14	4.0
14		0.059	73	9.5	-43	3.1	24		1.1	21	ND	-35	4.9
15		0.26	32	9.1	-39	5.5							

^aSC_{1.5}: compound concentration required to achieve GK activity 150% of control, numbers are the average from at least three independent assays, the average CV of the assay was 15% based on data analysis of over 400 compounds with SC_{1.5} < 2 μM. ^bPercentage of inhibition of hERG potassium channel at a compound concentration of 10 μM; numbers are the average from at least three measurements. ^cTime-dependent inactivation (TDI) of CYP3A4 at a compound concentration of 10 μM after 24 min of incubation; numbers are the average from three measurements. ^dBlood glucose change (%) compared to vehicle at the 4 h time point after C57 mice were orally dosed with compound (50 mg/kg). ^eLipophilic ligand efficiency (LLE) calculated as (pSC_{1.5} - clogP).

Information, indicated that the α -substituted phenylacetic acid in **1** was the optimized fragment. Therefore, this moiety was maintained, and our lead optimization was focused on the aminopyrazine fragment. We envisioned that adding polar groups to the 5-position of the 2-aminopyrazine in **1** could reduce or eliminate the liabilities of CYP3A4 TDI and hERG inhibition without sacrificing activator potency. To this end, a series of 5-substituted-2-aminopyrazine-derived GK activators were synthesized, and these compounds (**4** and **9–24**) were assayed for their GK activation potency and their liability in inactivating human CYP3A4 at a compound concentration of 10 μM. The effects of GK activators on the hERG potassium channel were assessed using the patch clamp method, and dose-dependent hERG inhibition was measured. Our goal was to achieve a hERG IC₂₀ value around 10 μM. Therefore, the

percentage of hERG inhibition at a compound concentration of 10 μM is listed in Table 1. Furthermore, these compounds were evaluated for their ability to lower blood glucose in C57 mice in comparison with vehicle dosing as listed in Table 1. As an indication of improvement in the physicochemical properties of these compounds, the lipophilic ligand efficiency (LLE) values are also listed.¹⁴

As shown in Table 1, the 5-position of aminopyrazine-derived GKAs can tolerate a large variety of functional groups.¹⁵ Except for **6**, **9**, and **14**, all compounds achieved an improvement in LLE, and 5 of them displayed an increase of LLE greater than 1.0 when compared with **1** (**13**, **15**, **16**, **20**, and **4**). It is also important to note that the diol stereochemistry affected GK activation potency. The analogue with an (S)-configuration exhibited four times higher potency than the

corresponding (*R*)-configuration analogue (compare **4** with **24**), which is significant in our assay. However, this chemical series (except for **7**) appears to possess a strong hERG interaction pharmacophore and achieving a hERG IC₂₀ value less than 10 μM turned out to be challenging. Within the data set in Table 1, only five diol-derived activators displayed hERG inhibition about 20% at 10 μM (**11**, **12**, **4**, **22**, and **24**). In general, carboxylic acids carry a lower hERG inhibition liability. However, activators from aminopyridine- or aminopyrazine-derived carboxylic acids in our phenylacetamide chemical series did not demonstrate significant acute in vivo efficacy in lowering blood glucose (data not shown). With regard to CYP3A4 TDI, 8 compounds in Table 1 had a measured TDI value less than 20% at the concentration of 10 μM. Interestingly, replacing the methyl sulfide with the methyl sulfoxide completely removed TDI of CYP3A4 (compare **9** with **10**), while the two diol derivatives with alkoxy substitutions (**11** and **12**) still showed TDI greater than 20%.

To study the acute glucose lowering efficacy of GK activators in C57Bl/6J mice, animals (2 months old, *n* = 6 per dose group, fasted for 2 h prior to oral dosing) were orally treated with **1**, **4**, **7**, and **9–24** (50 mg/kg) or vehicle, and blood samples were taken every two hours post dosing (2, 4, 6, and 8 h time points). Changes in blood glucose levels compared to vehicle treatment at the 4 h time point are listed in Table 1. Except for **7**, all efficacy data in Table 1 achieved statistical significance (*p* < 0.01 for **1**, **4**, **9–22**, and **24**; *p* = 0.038 for **23**). As shown in the list, 11 compounds achieved glucose lowering greater than 40%. The indicated hypoglycemic effects of these compounds in C57 mice could be due to the relatively high dose.

By analyzing the data for hERG inhibition (20% @ 10 μM), CYP3A4 TDI (<20% @ 10 μM), in vitro GK activation (SC_{1.5} < 0.50 μM), and in vivo acute glucose lowering (>30% @ 50 mg/kg) in Table 1, we concluded that both **4** and **22** satisfied our criteria for compound selection. After investigation of different crystallization methods, the crystalline form of nonsolvated **4** was obtained. However, we did not obtain a crystalline form of **22**. Therefore, **4** was selected as a preclinical lead molecule.

We next characterized the kinetic properties of GK at different concentrations of **4**. Enzymatic assays using recombinant human GK indicated dose-dependent GK activation by **4** at all glucose concentrations (Figure S1 in Supporting Information). The enzyme kinetic profile of **4** demonstrated the ability of the compound to increase enzyme *V*_{max} from 10.0 μM/min to 16.0 μM/min (1.6 fold) and decrease substrate SC_{0.5} (glucose concentration to reach half of the *V*_{max}) from 7.5 to 3.9 mM.

To further investigate **4** for its potential as an oral antidiabetic agent, we studied **4** for drug-like properties. As listed in Table 2A, **4** displayed good solubility and permeability, with a hERG IC₅₀ value greater than 50 μM. The desirable physicochemical properties of **4** prompted us to investigate its pharmacokinetic profiles in mice and dogs. As listed in Table 2B, good oral bioavailability was achieved in C57 mice and dogs.

Encouraged by the pharmacokinetic profiles of **4**, we further assessed its dose-dependent efficacy on lowering glucose in diet-induced obesity (DIO) mice. As shown in Figure 2, dose-dependent lowering of blood glucose was observed after DIO mice (*n* = 9 per dose, C57Bl/6J mice, 6 months old, on a high-fat diet for 4 months) were orally treated with **4** (7.5, 15, and 30 mg/kg). At the time point of 2 and 4 h post oral dosing,

Table 2. (A) Physicochemical and in vitro predictive safety profiles of **4**; (B) Pharmacokinetic properties of **4** in mouse and dogs

A. properties		results			
log <i>D</i> (pH = 7.4)		2.7			
solubility (pH = 7.4)		0.17 mg/mL			
<i>pK</i> _a		11.42			
caco-2 permeability (Papp)		3.36 × 10 ⁻⁶ cm/s			
human plasma protein binding (unbound <i>F</i> _u)		10%			
hERG IC ₅₀		70 μM			
CYP (7 CYP isoforms) IC ₅₀		>30 μM			
covalent binding to human liver microsomes (30 min, with NADPH)		33 pmol/mg protein			
B. species		mouse		dog	
route		iv	po	iv	po
dose (mg/kg)		10	30	10	30
Cl (mL/min/kg)		20.8		8	
<i>V</i> _{ss} (L/kg)		1.44		1.69	
AUC _{0-inf} (ng hr/mL)		8,010	12100	21600	54500
<i>C</i> _{max} (ng/mL)		1310		3790	
<i>t</i> _{max} (h)		4		7.3	
oral bioavailability (%)		50.3		84	

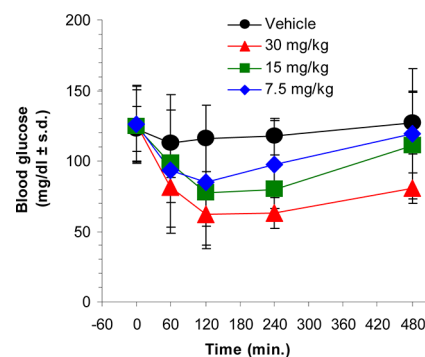
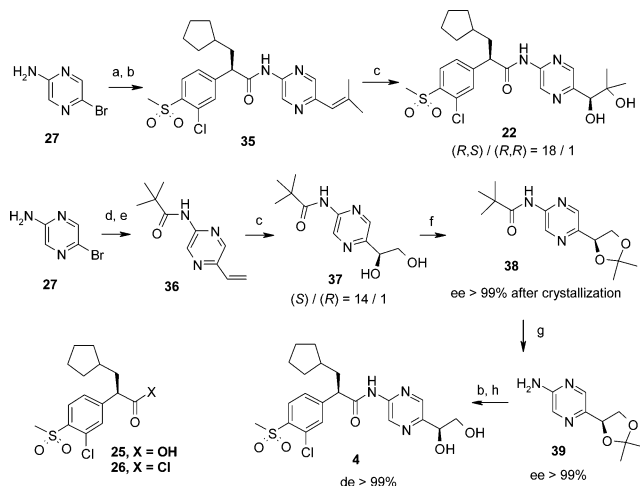


Figure 2. Compound **4** lowers basal glucose in DIO mice.

compound **4** (30 mg/kg) lowered basal glucose by 45% (*p* < 0.001). Even at the lower dose (15 mg/kg), compound **4** was able to lower glucose levels at the 2 and 4 h time points by 32% (*p* < 0.02), with an ED₂₅ value of 10 mg/kg. A good correlation of drug exposure level to blood glucose lowering was obtained (Table S2 in Supporting Information).

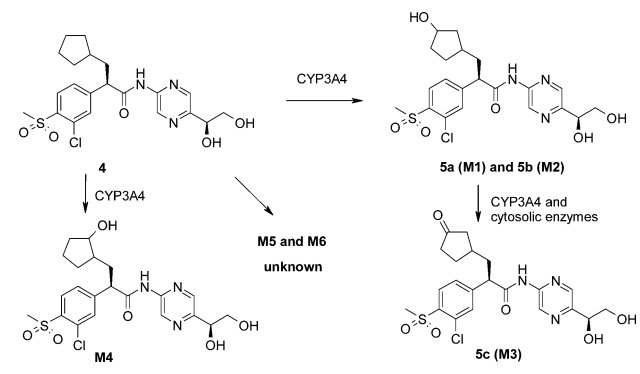
The syntheses of **1**, **7**, **8**, and the required left-hand piece **25** were carried out according to our earlier reported method.¹³ The starting material for compound **6** was prepared through the nucleophilic substitution of **25** with sodium methoxide. The synthetic schemes for the preparation of GKAs **9–21** and **23** including the intermediates are described in the Supporting Information. The syntheses of **4** and **22** using the Sharpless asymmetric dihydroxylation reaction¹⁶ are detailed in Scheme 1. The key step is the enantiomeric enrichment of the diol through the crystallization of the corresponding acetonide **38**. This route allowed our medicinal chemistry lab to prepare a large batch (200 g) of **4** for dose range finding studies.

To demonstrate that the issue of metabolite cycling was resolved with **4**, the ¹⁴C-labeled compound was incubated with liver microsomes and hepatocytes from multiple species, and the in vitro phase-1 metabolite pathway is described in Scheme 2. Unlike **2**, which displayed significant ketone reduction in human hepatocytes (35%, Table S3 in Supporting Information; metabolism pathway for **2** has been reported¹³), **4** demon-

Scheme 1. Syntheses of 22 and the Clinical Lead 4^a

^aReagents and conditions: (a) Pd(PPh₃)₄ (cat), tributyl-(2-methylpropenyl)stannane, EtNPr₂, LiCl, DMF, 130 °C; (b) compound 26, pyridine, CH₂Cl₂; (c) K₃Fe(CN)₆, K₂CO₃, hydroquinone 1,4-phthalazinediyl diether (cat), OsO₄ (cat), *t*-BuOH/H₂O, 0 °C, 18 h; (d) pivaloyl chloride, pyridine, CH₂Cl₂; (e) potassium vinyltrifluoroborate, 1,1'-bis(diphenylphosphino)ferrocene palladium dichloride, ethanol, 100 °C; (f) 2,2-dimethoxypropane, *p*-toluene sulfonic acid (cat), THF; (g) K₂CO₃, MeOH; (h) 2 N HCl (aq), THF.

Scheme 2. In Vitro Phase-1 Metabolism Pathway of 4 in Liver Microsomes and Hepatocytes



strated high stability (95%, Table S4 in Supporting Information). A metabolism study of 4 with human liver microsomes (Table S5 in Supporting Information) indicated minimal formation of ketone 5c (M3) by further oxidation of the alcohols 5a and 5b.

We previously reported compound 2 as the first GK activator to reach the clinic. However, this molecule was stopped at the phase 2 stage due to transient mild elevation of liver enzymes in a very small percentage of patients. The mechanism for the clinical observation remains unclear. One possibility is that parent/metabolite cycling placed abnormal stress on the liver. The successful resolution of metabolite cycling allowed us to select 4 as a backup molecule to 2. Following thorough preclinical safety assessment, 4 advanced to clinical testing in type 2 diabetic patients.

The analysis of clinical data confirmed the significantly different metabolite profile between 4 and 2 (Figure S2 in Supporting Information). The parent ketone 2 and its metabolite alcohol 3 showed comparable C_{max} , with slightly higher exposure for the metabolite 3 than the parent following

a single oral dose of 100 mg in diabetic patients, which is consistent with the metabolite cycling observed in metabolism studies. However, the monohydroxylated forms 5a and 5b exhibited significantly lower C_{max} and exposure than the parent 4. The ketone, 5c, had the lowest exposure compared with the parent and the monohydroxylated forms. The metabolite to parent ratio for 2, [3]/[2], is 0.74 as calculated by C_{max} and 1.39 as calculated by AUC. The corresponding ratios for 4 are significantly lower (Table S6 in Supporting Information). The low level of ketone 5c (4% of the parent by C_{max}) suggests that the potential for redox cycling has been significantly decreased.

In summary, we discovered a novel GK activator 4. This diol-containing molecule showed improved lipophilic ligand efficiency (LLE = 5.6) compared to the lead 1 (LLE = 4.0). In the clinic, no evidence of metabolic cycling was seen in contrast to observations from the previous clinical GKA, 2. The lead optimization approach we took underscores the importance of improving physicochemical properties in drug design. The unique feature of the diol fragment to modulate molecular properties paved the way for our further discovery of potent and efficacious GKAs from other chemical scaffolds.^{17,18}

■ ASSOCIATED CONTENT

S Supporting Information

Detailed synthetic schemes for the synthesis of 9–21 and 23, experimental procedures, preclinical data (Figure S1, Table S1–S5), and clinical data (Figure S2 and Table S6). This material is available free of charge via the Internet at <http://pubs.acs.org>.

■ AUTHOR INFORMATION

Corresponding Author

* (Y.Q.) Tel: 973-235-3240. E-mail: yiminqian81@gmail.com.

Notes

The authors declare no competing financial interest.

■ ACKNOWLEDGMENTS

We gratefully acknowledge Margret Jonca for chiral HPLC analysis; Gino Sasso for ¹H NMR characterization of metabolites; Bruce Banner, Fred Bizzarro, Shaoqing Chen, Steven Mischke, Lida Qi, and Kshitij Thakkar for chemistry contributions; formulation, drug metabolism, and toxicology groups for their support; Jefferson Tilley, Nader Fotouhi, Joseph Grippo, and Rebecca Taub for project guidance; and Karen Lackey for the management support of manuscript preparation.

■ REFERENCES

- (1) Matschinsky, F. M. Assessing the potential of glucokinase activators in diabetes therapy. *Nat. Rev. Drug Discovery* 2009, 8, 399–416.
- (2) Grimsby, J.; Sarabu, R.; Corbett, W. L.; Haynes, N. E.; Bizzarro, F. T.; Coffey, J. W.; Guertin, K. R.; Hilliard, D. H.; Kester, R. F.; Mahaney, P. E.; Marcus, L.; Qi, L.; Spence, C. L.; Tengi, J.; Magnuson, M. A.; Chu, C. A.; Dvorozniak, M. T.; Matschinsky, F. M.; Grippo, J. F. Allosteric activators of glucokinase: potential role in diabetes therapy. *Science* 2003, 301, 370–373.
- (3) Haynes, N. E.; Corbett, W. L.; Bizzarro, F. T.; Guertin, K. R.; Hilliard, D. W.; Holland, G. W.; Kester, R. F.; Mahaney, P. E.; Qi, L.; Spence, C. L.; Tengi, J.; Dvorozniak, M. T.; Raikar, A.; Matschinsky, F. M.; Grippo, J. F.; Grimsby, J.; Sarabu, R. Discovery, structure–activity relationships, pharmacokinetics, and efficacy of glucokinase activator (2*R*)-3-cyclopentyl-2-(4-methanesulfonylphenyl)-*N*-thiazol-2-yl-propionamide (RO0281675). *J. Med. Chem.* 2010, 53, 3618–3625.

(4) McKerrecher, D.; Allen, J. V.; Caulkett, P. W. R.; Donald, C. S.; Fenwick, M. L.; Grange, E.; Johnson, K. M.; Johnstone, C.; Jones, C. D.; Pike, K. G.; Rayner, J. W.; Walker, R. P. Design of a potent, soluble glucokinase activator with excellent in vivo efficacy. *Bioorg. Med. Chem. Lett.* **2006**, *16*, 2705–2709.

(5) (a) Waring, M. J.; Johnstone, C.; McKerrecher, D.; Pike, K. G.; Robb, G. Matrix-based multiparameter optimization of glucokinase activators: the discovery of AZD1092. *Med. Chem. Commun.* **2011**, *2*, 775–779. (b) Waring, M. J.; Clarke, D. S.; Fenwick, M. D.; Godfrey, L.; Groombridge, S. D.; Johnstone, C.; McKerrecher, D.; Pike, K. G.; Rayner, J. W.; Robb, G. R.; Wilson, I. Property based optimization of glucokinase activators: discovery of phase IIB clinical candidate AZD1656. *Med. Chem. Commun.* **2012**, *3*, 1077–1081.

(6) Mao, W.; Ning, M.; Liu, Z.; Zhu, Q.; Leng, Y.; Zhang, A. Design, synthesis, and pharmacological evaluation of benzamide derivatives as glucokinase activators. *Bioorg. Med. Chem.* **2012**, *20*, 2982–2991.

(7) Meininger, G. E.; Scott, R.; Alba, M.; Shentu, Y.; Luo, E.; Amin, H.; Davies, M. J.; Kaufman, K. D.; Goldstein, B. J. Effects of MK-0941, a novel glucokinase activator, on glycemic control in insulin-treated patients with type 2 diabetes. *Diabetes Care* **2011**, *34*, 2560–2566.

(8) Takahashi, K.; Hashimoto, N.; Nakama, C.; Kamata, K.; Sasaki, K.; Yoshimoto, R.; Ohyama, S.; Hosaka, H.; Maruki, H.; Nagata, Y.; Eiki, J. I.; Nishimura, T. The design and optimization of a series of 2-(pyridin-2-yl)-1H-benzimidazole compounds as allosteric glucokinase activators. *Bioorg. Med. Chem.* **2009**, *17*, 7042–7051.

(9) Nishimura, T.; Iino, T.; Mitsuya, M.; Bamba, M.; Watanabe, H.; Tsukahara, D.; Kamata, K.; Sasaki, K.; Ohyama, S.; Hosaka, H.; Futamura, M.; Nagata, Y.; Eiki, J. I. Identification of novel and potent 2-amino benzamide derivatives as allosteric glucokinase activators. *Bioorg. Med. Chem. Lett.* **2009**, *19*, 1357–1360.

(10) Bertram, L. S.; Black, D.; Briner, P. H.; Chatfield, R.; Cooke, A.; Fyfe, M. C. T.; Murray, P. J.; Naud, F.; Nawano, M.; Procter, M. J.; Rakipovski, G.; Rasamison, C. M.; Reynet, C.; Schofield, K. L.; Shah, V. K.; Spindler, F.; Taylor, A.; Turton, R.; Williams, G. M.; Wong-Kai-In, P.; Yasuda, K. SAR, pharmacokinetics, safety, and efficacy of glucokinase activating 2-(4-sulfonylphenyl)-N-thiazol-2-ylacetamides: discovery of PSN-GK1. *J. Med. Chem.* **2008**, *51*, 4340–4345.

(11) Bebernitz, G. R.; Beaulieu, V.; Dale, B. A.; Deacon, R.; Duttaroy, A.; Gao, J.; Grondine, M. S.; Gupta, R. C.; Kakmak, M.; Kavana, M.; Kirman, L. C.; Liang, J.; Maniara, W. M.; Munshi, S.; Nadkarni, S. S.; Schuster, H. F.; Stams, T.; St. Denny, I.; Taslimi, P. M.; Vash, B.; Caplan, S. L. Investigation of functionally liver selective glucokinase activators for the treatment of type 2 diabetes. *J. Med. Chem.* **2009**, *52*, 6142–6152.

(12) Pfefferkorn, J. A.; Guzman-Perez, A.; Litchfield, J.; Aiello, R.; Treadway, J. L.; Pettersen, J.; Minich, M. L.; Filipowski, K. J.; Jones, C. S.; Tu, M.; Aspnes, G.; Risley, H.; Bian, J.; Stevens, B. D.; Bourassa, P.; D'Aquila, T.; Baker, L.; Barucci, N.; Robertson, A. S.; Bourbonais, F.; Derksen, D. R.; MacDougall, M.; Cabrera, O.; Chen, J.; Lapworth, A. L.; Landro, J. A.; Zavadski, W. J.; Atkinson, K.; Haddish-Berhane, N.; Tan, B.; Yao, L.; Kosa, R. E.; Varma, M. V.; Feng, B.; Duignan, D. B.; El-Kattan, A.; Murdande, S.; Liu, S.; Ammirati, M.; Knafels, J.; DaSilva-Jardine, P.; Sweet, L.; Liras, S.; Rolph, T. P. Discovery of (S)-6-(3-cyclopentyl-2-(4-(trifluoromethyl)-1H-imidazol-1-yl)propanamido)-nicotinic acid as a hepatoselective glucokinase activator clinical candidate for treating type 2 diabetes mellitus. *J. Med. Chem.* **2012**, *55*, 1318–1333.

(13) Sarabu, R.; Bizzarro, F. T.; Corbett, W. L.; Dvorozniak, M. T.; Geng, W.; Grippo, J. F.; Haynes, N. E.; Hutchings, S.; Garofalo, L.; Guertin, K. R.; Hilliard, D. W.; Kabat, M.; Kester, R. F.; Wang, K.; Liang, Z.; Mahaney, P. E.; Marcus, L.; Matschinsky, F. M.; Moore, D.; Racha, J.; Radinov, R.; Ren, Y.; Qi, L.; Pignatello, M.; Spence, C. L.; Steele, T.; Teng, J.; Grimsby, J. Discovery of Piragliatin-first glucokinase activator studied in type 2 diabetic patients. *J. Med. Chem.* **2012**, *55*, 7021–7036.

(14) Meanwell, N. A. Improving drug candidates by design: a focus on physicochemical properties as a means of improving compound disposition and safety. *Chem. Res. Toxicol.* **2011**, *24*, 1420–1456.

(15) Chen, S.; Corbett, W. L.; Guertin, K. R.; Haynes, N.; Kester, R. F.; Mennona, F. A.; Mischke, S. G.; Qian, Y.; Sarabu, R.; Scott, N. R.; Thakkar, K. C. 5-Substituted-Six-Membered Heteroaromatic Glucokinase Activators. U.S. Patent 7,132,425, 2006.

(16) Kolb, H. C.; VanNieuwenhze, M. S.; Sharpless, K. B. Catalytic asymmetric dihydroxylation. *Chem. Rev.* **1994**, *94*, 2483–2547.

(17) Berthel, S. J.; Brinkman, J. A.; Hayden, S.; Haynes, N. E.; Kester, R. F.; McDermott, L. A.; Qian, Y.; Sarabu, R.; Scott, N. R.; Tilley, J. W. Pyrrolidinone Glucokinase Activators. U.S. Patent 7,741,327, 2010.

(18) Berthel, S. J.; Haynes, N. E.; Kester, R. F.; McDermott, L. A.; Qian, Y.; Sarabu, R.; Scott, N. R.; Tilley, J. W. Pyridazinone Glucokinase Activators. U.S. Patent 8,258,134, 2012.